Available online at www.sciencedirect.com
SCIENCE DIRECT®
International Journal of Mass Spectrometry 229 (2003) 151–156
International Journal of Mass Spectrometry
www.elsevier.com/locate/ijms

Electron impact ionization of the Cl_2 molecule

Satyendra Pal*, P. Bhatt, J. Kumar

Department of Physics, Janta Vedic College (C.C.S. University, Meerut) Baraut 250 611, Baghpat, U.P., India

Received 13 January 2003; accepted 3 June 2003

Abstract

The single, double and triple differential cross-sections at 100 eV for the production of the Cl_2^+, Cl^+ and Cl_2^{2+} ions from electron impact ionization of the Cl_2 molecule have been evaluated using a semi-empirical model. The partial ionization cross-sections have also been derived with incident electron energies varying from ionization threshold to 200 eV.

Keywords: Ionization; Differential cross-section; Electron impact; Chlorine molecule

1. Introduction

Molecular chlorine (Cl_2) is a plasma processing gas. It is used in plasma etching of semiconductors where the Cl atoms produced in a gas discharge through the dominant processes, dissociative and non-dissociative ionization efficiently etch a silicon surface. The ionization cross-section data quantifying the consequences of the electron interaction with Cl_2 is essential for modeling of chlorine plasmas to gain a more detail understanding of the etching process [1,2]. Molecular chlorine is also of atmospheric and environmental interest. It is a potential atmospheric reservoir of Cl atoms, which are released photolytically [3,4].

An early attempt to critically evaluate low energy electron impact cross-section data for Cl_2 was made by Morgan [5]. However, recently assembled library of data quantifying the electron-Cl_2 collision by Christophorou and Olthoff [6] are provided a vital step towards the understanding of electron ionization mechanism of Cl_2. The partial photo-ionization cross-sections were measured by Samson and Angle [7] in the photon energy range from ionization threshold (onset values) to 80 eV. The electron impact total ionization cross-sections (TICS) include the measurements of Center and Mandl [8], Kurepa and Belić [9], Stevie and Vasile [10] and Srivastava [11]. Calandra et al. [12] have provided the quantitative experimental information on the relative partial ionization cross-sections for various types of ions formed via, single, double dissociative and triple dissociative ionization of the Cl_2 molecule by electron impact.

On the other hand, rigorous quantum mechanical approach for the calculation of electron ionization cross-sections for molecules is limited to the application of simple molecules. Contrary to it, there now exist semi-classical and semi-empirical models including Deutsch and Märk (DM) formulation [13], binary encounter Bethe formulation of Kim and co-workers [14] and Jain–Khare formulation based on the Bethe and Möller cross-sections [15–17]. However, recently, Kim and Deutsch et al. (see for instance ref. [11]) have evaluated the TICS by employing their respective theoretical models. The model dependent TICS were also deduced by Rogoff et al. [18] and Pinhão and Chouki [19] from the modeling of the chlorine discharge. Most recently, Joshipura and Limbachyia [20] have computed the TICS using modified additive approach based on complex potential.

In the present work, we have employed the modified Jain–Khare semi-empirical formulation [21–23] to evaluate the partial ionization cross-sections for Cl_2 by electron impact. The three channels direct or non-dissociative, dissociative and double ionization (DI) leading to the production of Cl_2^+, Cl^+ and Cl_2^{2+} ions, respectively, have been considered. For the first time, the single differential cross-sections (SDCS) (function of secondary electron energy), double differential cross-sections (DDCS) (function of secondary electron energy and the scattering angle) and triple differential cross-sections (TDCS) (function of secondary electron energy, scattering angle and tertiary electron energy)

* Corresponding author. Tel.: +91-1234-262014; fax: +91-1234-262130.
E-mail address: satyendrapal1@rediffmail.com (S. Pal).

1387-3806/$ – see front matter © 2003 Elsevier B.V. All rights reserved.
doi:10.1016/S1387-3806(03)00301-4

corresponding to the production of different ions have been evaluated at incident electron energy of 100 eV. The partial integral ionization cross-sections (PICS) and the TICS, i.e., the sum of PICS, are also derived with incident electron energies varying from ionization threshold to 200 eV. To the best of our knowledge, no experimental data is available to compare the present results except for TICS. A comparison of our total PICS with the available various experimental and theoretical data [8–11,18–20] including the suggested and recommended data by Christophorou and Olthoff [6] revealed a satisfactory agreement.

2. Theoretical

Recently, the present formulation has been employed to evaluate the single and double differential cross-sections for several molecules over a wide range of incident electron energy [21–24]. Here we have employed this approach with certain modifications to evaluate the triple differential cross-sections along-with the partial single and double differential cross-sections for the chlorine molecule. According to the present form of the semi-empirical formulation, the SDCS for the production of secondary electron of energy ε corresponding to the production of ith type of ion in the ionization of a molecule by an incident electron of energy E is given by

$$Q_i(E, W) = Q_i^{\mathrm{B}}(E, W) + Q_i^{\mathrm{M}}(E, W) \tag{1}$$

with the Bethe part

$$Q_i^{\mathrm{B}}(E, W) = \frac{4\pi a_0^2 R^2}{E}\left[\frac{1}{(1+(I_i/E))}\left(1-\frac{\varepsilon}{(E-I_i)}\right) \times \frac{1}{W}\frac{\mathrm{d}f_i(W,0)}{\mathrm{d}W}\ln[1+C_i(E-I_i)]\right] \tag{1a}$$

and the Mott part

$$Q_i^{\mathrm{M}}(E, W) = \frac{4\pi a_0^2 R^2}{E}\left[S_i\frac{(E-I_i)}{E(\varepsilon^3+\varepsilon_0^3)}\left(\varepsilon-\frac{\varepsilon^2}{(E-\varepsilon)}+\frac{\varepsilon^3}{(E-\varepsilon)^2}\right)\right] \tag{1b}$$

where $W\,(=\varepsilon+I_i)$ is the energy loss suffered by the primary electron. I_i, a_0, C_i and R are the ionization threshold for the production of ith type of ion, first Bohr's radius, collision parameter and the Rydberg's constant, respectively. It is remarkable to note that the factor $(1+I_i/E)$ appeared in the Bethe part of Eq. (1) ignored in the previous calculations of PICS and DCS (see ref. [15] for detail), played an important role at low and intermediate energy regimes and hence is considered in the present work. This could reveal a significant improvement (∼10%) of cross-sections discussed in Section 3.

It is interesting to note that the second-fold differential cross-section is isotropic in nature and hence the molecular property defined in terms of the differential optical oscillator strength $\mathrm{d}f_i(W,0)/\mathrm{d}W$ must be angular dependent. In the present calculations of DDCS, we have used the three-fold differential oscillator strengths (3DOS) in the Bethe regime (where momentum transfer $K \to 0$) [22]:

$$\lim_{K\to 0}\frac{\mathrm{d}f_i^3(W,K,\theta)}{\mathrm{d}W\,\mathrm{d}K\,\mathrm{d}\theta} = \frac{1}{4\pi}[1+\beta P_2(\cos\theta)]\frac{\mathrm{d}f_i(W,0)}{\mathrm{d}W} \tag{2}$$

where β, the asymmetric parameter is a function of secondary electron energy ε and is nothing but the transition probability S_i (probability of ionizable electrons). $P_2(\cos\theta)$, the second order Legendre polynomial is defined as $1/2(3\cos^2\theta-1)$. Thus, the second-fold or DDCS is defined as the differential of Eq. (1) with respect to the solid angle $\mathrm{d}\Omega = 2\pi\sin\theta\,\mathrm{d}\theta$. Where θ is the scattering angle:

$$Q_i(E, W, \theta) = \frac{\mathrm{d}Q_i(E, W)}{\mathrm{d}\Omega} \tag{3}$$

In $(e, 3e)$ processes where Cl_2^{2+} ions are formed, the three outgoing electrons, though indistinguishable, are indexed and discriminated by energy labels $(E-W)$ for the most forward "scattered" one and ε and ξ for two "ejected" ones. The three-fold or the TDCS, $Q_i(E, \varepsilon, \theta, \xi)$ is evaluated by the differentiation of Eq. (3) with respect to ξ, the energy of the ejected second electron:

$$Q_i(E, \varepsilon, \theta, \xi) = \frac{\mathrm{d}Q_i(E, W, \theta)}{\mathrm{d}\xi} \tag{4}$$

The total energy loss in $(e, 3e)$ process is defined as $W = I_i + \varepsilon + \xi$. Treating $(I_i + \varepsilon)$ a constant, one gets $\mathrm{d}W = \mathrm{d}\xi$.

The partial integral ionization cross-section is derived by the integration of SDCS in Eq. (1) over the entire energy loss W, i.e.,

$$Q_i(E) = \int_{I_i}^{W_{\max}=E} Q_i(E, W)\,\mathrm{d}W \tag{5}$$

The present formulation requires the major input data of the optical oscillator strengths $\mathrm{d}f_i(W,0)/\mathrm{d}W$ for the production of ith type of ions. These values are derived from the highly accurate (∼10% uncertainty) photo-ionization cross-sections Q_i^{ph}, measured by Samson and Angel [7] from vertical ionization threshold (onset values) to 80 eV of photon energies:

$$Q_i^{\mathrm{ph}}(mb) = 109.75\frac{\mathrm{d}f_i(W,0)}{\mathrm{d}W} \tag{6}$$

The vertical ionization threshold values corresponding to the production of ith type ions are compiled elsewhere [7]. For higher photon energies (>80 eV), we have used the extrapolated photo-ionization cross-sections. It is assumed that the error in the extrapolated region is the same as in the measurement of Q_i^{ph}. The typical parameter C, derived from the plot of TICS (accuracy of ∼95%) at high energies versus $\ln E$ with constant values of $(M_i^2/C)(=0.1)$ (the best fit value among 0.08–0.12) [25] have been employed using the

method developed earlier [16]. The value of mixing parameter ε_0 (=50 eV) as for other diatomic molecules [21–24,26] is used in the present evaluations. In our calculations the estimated error is more or less the same as in the measurement of Q_i^{ph}. In the present study, the ith values 1, 2 and 3 correspond to the production of Cl_2^+, Cl^+ and Cl_2^{2+} ions from electron-Cl_2 ionization.

3. Results and discussion

In Fig. 1a and b, we have presented the SDCS and DDCS at incident electron energy of 100 eV. The SDCS and DDCS are shown in the complete range of energy loss $W = (I_i + \varepsilon + \xi)$ varying from 0 to E. The DDCS are computed at the scattering angle of 30°. The three-fold TDCS, $Q_i(E, \varepsilon, \theta, \xi)$ as a function of tertiary or the second ejected electron energies ξ at ($E = 100$ eV, $\theta = 30°$ and $\varepsilon = 10$ and 20 eV) are presented in Fig. 1c. The numerical values of various differential cross-sections are also summarized in Table 1. To the best of our knowledge no data is available to compare the present calculated results. It is noted from the curves that the trends of the single and double differential cross-sections are the same as for other molecules [21–24] where theory and experiments are generally in agreement.

Fig. 2a and b with Table 2 depict the PICS leading to the production of parent ion Cl_2^+ and dissociative ions Cl^+ and Cl_2^{2+} through the electron-Cl_2 ionization. Recently, Calandra et al. [12] have measured the branching ratio Cl^+/Cl_2^+ which is much higher than the calculated ratio of cross-sections. In their experiments they have collected all Cl^+ ions produced through the different ionization processes, e.g., dissociative, double dissociative and ion-pair. The present calculations are based on the measured and normalized photo-ionization cross-sections corresponding to the direct, dissociative and direct double ionization processes [7]. In the absence of direct measurement for ionic cross-sections individually, the total PICS becomes important to compare with the available experimental and theoretical data standing for TICS. In Fig. 2b we have plotted only the recently evaluated TICS data including those of Kim and Deutsch et al. [11] and Joshipura and Limbachiya [20]. Recently, Christophorou and Olthoff [6] have analyzed and recommended TICS data within 20% uncertainty, which is an average of measured data of Kurepa and Belić [9] and Stevie and Vasile [10] hence it is not necessary to present these data independently along with the same data in the figure. The measured cross-sections by Srivastava [11] show structure near 25 eV, which although not as evident, is nonetheless indicated by some of the other measurements,

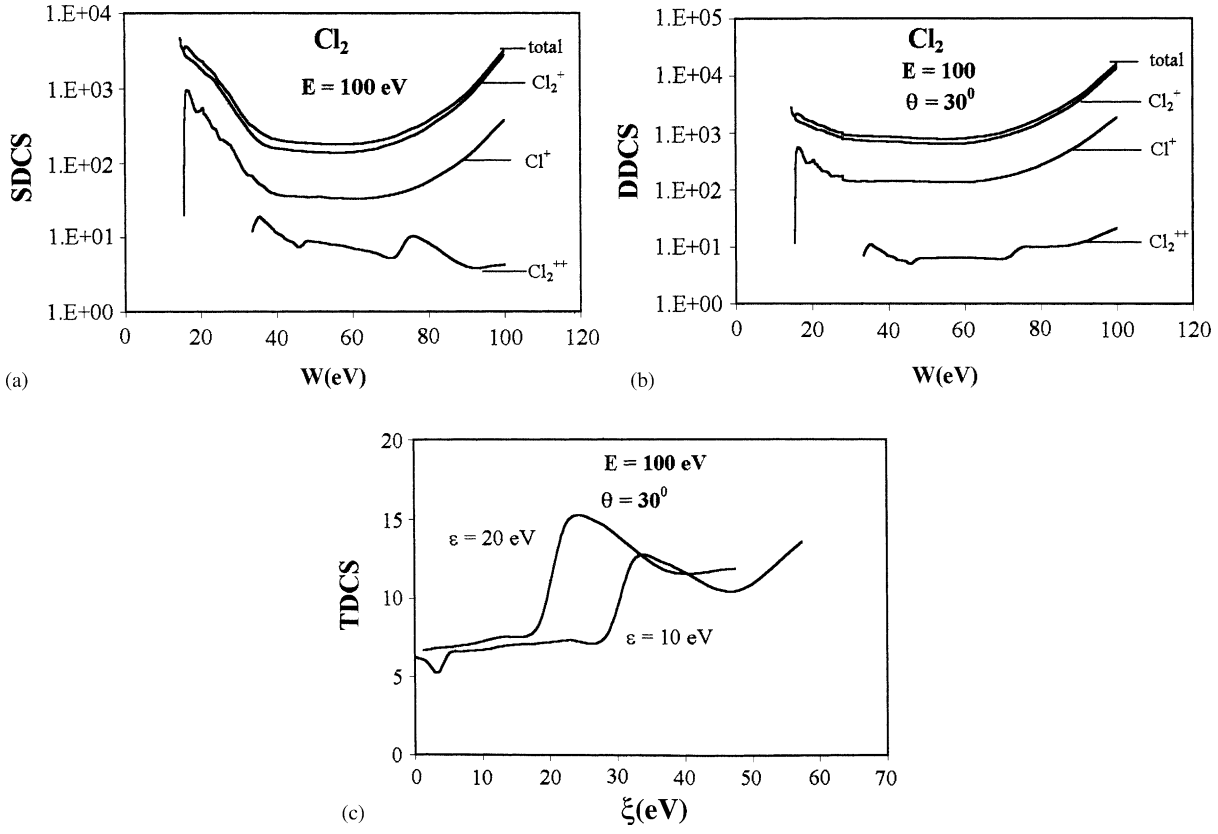

Fig. 1. (a) Solid curves represent the SDCS ($\times 10^{-20}$ cm^2/eV) as a function of energy loss W at $E = 100$ eV corresponding to the production of various ions from electron impact ionization of the Cl_2 molecule. (b) Similar to (a) but for DDCS ($\times 10^{-21}$ cm^2/eV-sr) at $E = 100$ eV and $\theta = 30°$. (c) Solid curves represent the TDCS ($\times 10^{-21}$ cm^2/eV^2-sr) as a function of tertiary electron energy ξ at $E = 100$ eV, $\theta = 30°$ and $\varepsilon = 10$ and 20 eV.

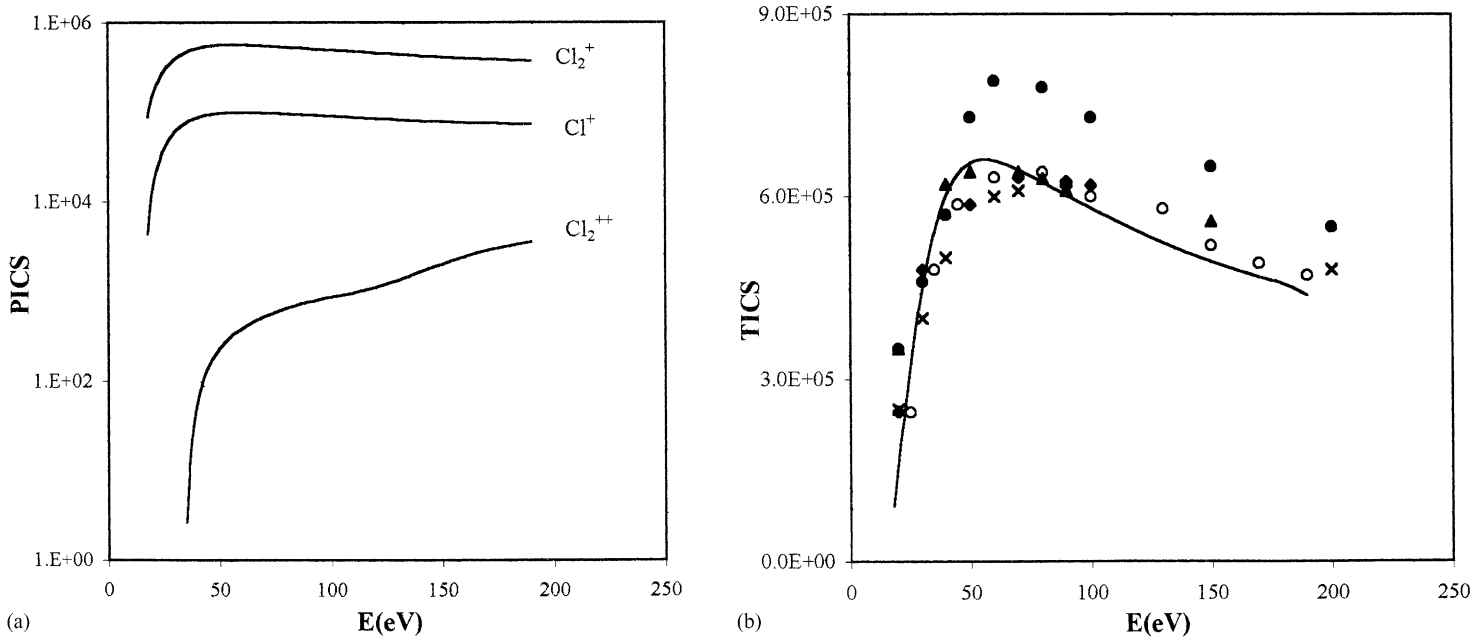

Fig. 2. (a) Solid curves represent the PICS ($\times 10^{-21}$ cm^2) as a function of incident electron energy corresponding to the production of ionic fragments from electron ionization of the Cl_2 molecule. (b) Solid curve represents the TICS ($\times 10^{-21}$ cm^2) as a function of incident electron energy. Data standing for TICS: (◆) recommended data by Christophorou and Olthoff [6], (●) Kim [11], (▲) Deutsch et al. [11], (×) Pinhão and Chouki [19], and (○) Joshipura and Limbachyia [20].

Table 1
(a) Single differential cross sections (SDCS) of the Cl_2 molecule

W (eV)	$Q_i(E, W)$ ($\times 10^{-20}$ cm^2/eV) $E = 100$ eV			
	Cl_2^+	Cl^+	Cl_2^{2+}	Total
15	3.63E+3			3.63E+3
20	1.88E+3	5.09E+2		2.38E+3
25	1.04E+3	2.26E+2		1.27E+3
30	3.62E+2	8.56E+1		4.48E+2
35	1.96E+2	5.17E+1	1.88E+1	2.66E+2
40	1.57E+2	3.81E+1	1.14E+1	2.07E+2
50	1.41E+2	3.45E+1	8.68E+0	1.84E+2
60	1.40E+2	3.30E+1	7.00E+0	1.80E+2
65	1.52E+2	3.37E+1	6.24E+0	1.92E+2
70	1.84E+2	3.76E+1	5.37E+0	2.27E+2
75	2.26E+2	4.40E+1	1.02E+1	2.80E+2
80	3.06E+2	5.64E+1	8.25E+0	3.71E+2
90	7.21E+2	1.19E+2	3.99E+0	8.44E+2

*a*E*b* stands for $a \times 10^b$.

(b) Double differential cross sections (DDCS) of the Cl_2 molecule

W (eV)	$Q_i(E, W, \theta)$ ($\times 10^{-21}$ cm^2/eV-sr) $E = 100$ eV, $\theta = 30^\circ$			
	Cl_2^+	Cl^+	Cl_2^{2+}	Total
15	2.17E+3			2.17E+3
20	1.27E+3	3.14E+2		1.59E+3
25	9.74E+2	1.81E+2		1.16E+3
30	7.74E+2	1.43E+2		9.17E+2
35	7.20E+2	1.41E+2	1.11E+1	8.72E+2
40	7.06E+2	1.42E+2	7.00E+0	8.56E+2
50	6.55E+2	1.39E+2	6.23E+0	8.00E+2
60	6.61E+2	1.37E+2	6.40E+0	8.05E+2
65	7.28E+2	1.46E+2	6.35E+0	8.81E+2
70	8.91E+2	1.71E+2	6.26E+0	1.07E+3
75	1.11E+3	2.06E+2	9.82E+0	1.33E+3
80	1.52E+3	2.72E+2	9.95E+0	1.80E+3
90	3.60E+3	5.91E+2	1.15E+1	4.20E+3

*a*E*b* stands for $a \times 10^b$.

(c) Triple differential cross sections (TDCS) of the Cl_2 molecule

$Q_i(E, \varepsilon, \theta, \xi)$ ($\times 10^{-21}$ cm^2/eV^2-sr) $E = 100$ eV, $\theta = 30^\circ$

$\varepsilon = 10$ eV		$\varepsilon = 20$ eV	
ξ (eV)	TDCS	ξ (eV)	TDCS
0.16	6.22	1.31	6.70
1.69	5.99	3.76	6.84
3.33	5.22	7.89	7.03
5.09	6.50	12.66	7.52
7.00	6.58	18.26	8.16
9.07	6.68	22.55	14.71
11.31	6.80	27.40	14.71
13.76	7.00	37.40	11.70
17.89	7.10	47.40	11.81
22.66	7.34		
28.26	7.52		
32.55	12.40		
37.40	12.15		
47.40	10.41		
57.40	13.50		

Table 2
PICS of the Cl_2 molecule

E (eV)	$Q_i(E)$ ($\times 10^{-21}$ cm^2)			
	Cl_2^+	Cl^+	Cl_2^{2+}	Total
20	1.50E+5	1.34E+4		1.63E+5
25	2.85E+5	3.77E+4		3.23E+5
30	3.90E+5	5.99E+4		4.50E+5
35	4.66E+5	7.55E+4	2.66E+0	5.41E+5
40	5.16E+5	8.62E+4	5.53E+1	6.02E+5
45	5.45E+5	9.27E+4	1.43E+2	6.38E+5
50	5.59E+5	9.61E+4	2.31E+2	6.55E+5
52	5.61E+5	9.70E+4	2.63E+2	6.59E+5
54	5.63E+5	9.76E+4	2.95E+2	6.61E+5
56	5.63E+5	9.80E+4	3.25E+2	6.61E+5
58	5.62E+5	9.82E+4	3.53E+2	6.61E+5
60	5.61E+5	9.83E+4	3.81E+2	6.59E+5
64	5.56E+5	9.80E+4	4.36E+2	6.54E+5
70	5.47E+5	9.71E+4	5.18E+2	6.44E+5
74	5.40E+5	9.62E+4	5.69E+2	6.37E+5
80	5.29E+5	9.47E+4	6.44E+2	6.24E+5
90	5.10E+5	9.21E+4	7.56E+2	6.03E+5
100	4.91E+5	8.95E+4	8.57E+2	5.82E+5
110	4.74E+5	8.69E+4	9.54E+2	5.61E+5
120	4.57E+5	8.44E+4	1.10E+3	5.42E+5
130	4.41E+5	8.20E+4	1.32E+3	5.25E+5
140	4.27E+5	7.97E+4	1.63E+3	5.08E+5
150	4.13E+5	7.78E+4	1.98E+3	4.93E+5
160	4.01E+5	7.61E+4	2.42E+3	4.80E+5
170	3.90E+5	7.47E+4	2.84E+3	4.78E+5
180	3.80E+5	7.35E+4	3.21E+3	4.70E+5
190	3.70E+5	7.24E+4	3.57E+3	4.68E+5

*a*E*b* stands for $a \times 10^b$.

and might be due to auto-ionization. For the sake of clarity, these cross-section values [11] are not presented in the figure. The model dependent TICS of Pinhão and Chouki [19] deduced from the modeling of chlorine is also supportive to our calculations and other experimental data. We have not included the similar calculations of Rogoff et al. [18] and the measurements of Center and Mandl [8] due to inconsistent shapes of their cross-sections.

In fact, it is well known that it is the correlation between the two target electrons, which is responsible for DI. The outer shell DI can be envisaged by either shake-off or two step process. The first one is three times larger than the second one [27]. In the present evaluation of differential cross-sections, we could not include the contribution of correlation effect. Moreover, the present calculations include the contribution of exchange effects through the Möller part of the formulation. In the measurement of dissociative and double ionization cross-sections, many experiments suffer mass discrimination effects and exchange effects. Different modes of normalization procedure adopted by the experimentalists also enhance the uncertainty in the data. It is evident from the comparison that our results for TICS are in good agreement (within experimental error bars) with most of the available experimental and theoretical data [6,11,19,20]. Moreover, the PICS and TICS satisfy the trivial requirements that the threshold and asymptotic behaviors of the cross-sections.

The areas of the SDCS curves in Fig.1a corroborate to PICS at 100 eV which justify the consistency requirement of the ionization cross-sections.

4. Conclusions

We have evaluated the single, double and triple differential cross-sections at impinging electron energy of 100 eV corresponding to the production of various ionic species via direct and dissociative ionization processes of electron-Cl_2 using a modified semi-empirical formulation. The partial and total integral ionization cross-sections are also derived with incident electron energies varying from ionization threshold to 200 eV. With the exception of limited measurements and calculations for TICS, no measurements and calculations are known to have been made so far for differential cross-sections and partial ionization cross-sections. Since the work is advance at differential level, it is concerned with only the raw data, which can be integrated to compare with the experimental work. Undoubtedly, the present work quantifying the study of ionic species in electron-Cl_2 collision as a function of energy, may play a significant role for filling up a gap in the understanding of electron interaction with the Cl_2 molecule.

Acknowledgements

S. Pal is thankful to DST for financial assistance with their grant no. SR/FTP/PS-70/2001. Partial financial support from UGC is also acknowledged. Authors wish to thank Professor J.K. Olthoff (NIST, Maryland, USA) for providing the useful literature. Authors are also thankful to the referees for their valuable suggestions.

References

[1] D.M. Manos, D.L. Flamm (Eds.), Plasma Etching, Academic Press, Boston, 1989.
[2] M.J. Kushner, J. Appl. Phys. 82 (1997) 5312.
[3] T.E. Graedel, P.J. Crutzen, Chemie der Atmosphare, Spektrum Akademischer, Heidelberg, 1994.
[4] H. Tawara, in: T. Watnable, I. Shimamura, S. Shimizu, Y. Itikawa (Eds.), Molecular Processes in Space, Plenum Publication, Japan, 1990.
[5] W.L. Morgan, Plasma Chem. Plasma Process. 12 (1992) 449.
[6] L.G. Christophorou, J.K. Olthoff, J. Phys. Chem. Ref. Data 28 (1999) 131.
[7] J.A.R. Samson, G.C. Angel, J. Chem. Phys. 86 (1987) 1814.
[8] R.E. Center, A. Mandl, J. Chem. Phys. 57 (1972) 4104.
[9] M.V. Kurepa, D.S. Belić, J. Phys. B11 (1978) 3719.
[10] F.A. Stevie, M.J. Vasile, J. Chem. Phys. 74 (1981) 5106.
[11] Recently in 1998 (then unpublished) the measurement of S.K. Srivastava and calculations made by Kim using Binary Encounter Bethe Theory and Deutsch et al. using (DM) formulations were analyzed and synthesized by Christophorou and Olthoff [6]. We have taken these data from the same.
[12] P. Calandra, C.S.S. O'Connor, S.D. Price, J. Chem. Phys. 112 (2000) 10821.
[13] H. Deutsch, K. Becker, S. Matt, T.D. Märk, Int J. Mass Spectrom. 197 (2000) 37 (and references therein).
[14] K.K. Irikura, Y.-K. Kim, M.A. Ali, J. Res. Natl. Inst. Stand. Technol. 107 (2002) 63 (and references therein).
[15] S.P. Khare, W.J. Meath, J. Phys. B20 (1987) 2101.
[16] S.P. Khare, S. Prakash, W.J. Meath, Int. J. Mass Spectrom. Ion Process. 88 (1989) 299.
[17] S.P. Khare, M.K. Sharma, S. Tomar, J. Phys. B32 (1999) 3141; Y.-K. Kim, M.E. Rudd, J. Phys. B33 (2000) 1981.
[18] G.L. Rogoff, J.M. Kramer, R.B. Piejak, IEEE Trans. Plasma Sci. PS-14 (1986) 103.
[19] N. Pinhão, A. Chouki, in: K.H. Becker, W.E. Carr, E.E. Kunhardt (Eds.), Proceedings of the XXII International Conference on Phenomena in Ionized Gasses, Hoboken, NJ, 31 July–4 August 1995, contributed paper 2 (1995) P5.
[20] K.N. Joshipura, C.G. Limbachyia, Int. J. Mass Spectrom. 216 (2002) 239.
[21] S. Pal, S. Prakash, Rapid Commun. Mass Spectrom. 12 (1998) 297.
[22] S. Pal, Chem. Phys. Lett. 308 (1999) 428.
[23] S. Pal, S. Prakash, S. Kumar, J. Electron Spectrosc. Relat. Phenom. 109 (2000) 227.
[24] S. Pal, J. Kumar, P. Bhatt, J. Electron Spectrosc. Relat. Phenom. 129 (2003) 35.
[25] F. Rieke, W. Prepejchal, Phys. Rev. A6 (1972) 1507.
[26] D.K. Jain, S.P. Khare, Ind. J. Pure Appl. Phys. 14 (1977) 201; J. Phys. B9 (1976) 1429.
[27] A. Lahmam-Bennani, A. Duguet, in: Proceedings of Sixth International Symposium on Correlations, Plarization in Electronic and Atomic Collisions and $(e, 2e)$ Reactions, 18–21 July 1991, Flinders University, Adelaide, Australia.